Spectroscopic study and structural characterization of a Li-related photoluminescence center in neutron-irradiated Si

F. Rodriguez,[1,2,*] G. Davies,[1] and E. C. Lightowlers[1]
[1]*Department of Physics, King's College London, Strand, London WC2R 2LS, United Kingdom*
[2]*DCITIMAC, Facultad de Ciencias, University of Cantabria, 39005 Santander, Spain*
(Received 22 February 2000)

We report on a new Li-related photoluminescence center with zero-phonon line at 879.3 meV. The center is created at 550–600 °C in the final stages of annealing out radiation-induced point defects in float-zone silicon. Isotope and chemical correlation data establish that the center contains Li and C atoms. The isotope shift from ^{6}Li to ^{7}Li, $\Delta E = E(^7\mathrm{Li}) - E(^6\mathrm{Li}) = 0.18$ meV, is similar, per Li atom, to that observed for other Li-related centers in silicon. Uniaxial stress measurements establish the symmetry as monoclinic I, with only small departures from trigonal symmetry. A simple method for the transition is introduced to fit simultaneously the energies, polarizations, and relative intensities of the stress-split components. The transition's dipole is shown to be close to a bonding direction in the plane perpendicular to the characteristic $\langle 110 \rangle$ axis of the monoclinic I center. The vibronic sideband is produced by coupling to modes of 16, 31, and 36 meV, with a Huang-Rhys factor $S = 1.1$. This value can be predicted simply from the uniaxial-stress data. The temperature dependence of the zero-phonon line can be fitted precisely using the spectrum of coupled phonons derived from the vibronic band shape, plus the approximation that the differences in frequencies of the phonons in the ground and excited electronic states are proportional to the phonon frequency. The luminescence from the center is reversibly quenched with increasing temperature, with an activation energy $E_a = 32 \pm 5$ meV, however, we show that this result does not arise from the excited state containing a shallow particle. Although the center is created at 600 °C, it is rapidly destroyed at room temperature through passivation by the capture of one mobile Li atom.

I. INTRODUCTION

Due to their high mobility, lithium and hydrogen are important impurities in silicon that can passivate many defects giving rise to different Li and H associated complexes.[1–15] In general, H-related defects have received considerable attention due to the role played by hydrogen in modifying the electrical and optical properties of semiconductors,[16] and are a current theme of interest. The ability of H to form complexes with different defects and impurities has been clearly evidenced in Si by the great number of known defects which in recent years have been shown to contain H.[14–16] This behavior suggests that similar phenomena could probably occur when the next high-mobile hydrogenic impurity, Li, is present in Si. Therefore research on Li-related defects in Si is attractive not only to explore the ability of Li as passivator, but also as a way to understand the formation and structure of analogous H-related centers.

Although many Li centers have been reported for many years in the literature,[2–12] the structural characterization for most of them still remains unknown. The reasons for this lack of structural information lie in the difficulties of obtaining suitable crystals doped with different isotopes and in understanding the chemical processes involved in the formation of the centers. Neutron or electron irradiation and subsequent annealing is an effective way to create defects in silicon.[9–17] The four-Li associated vacancy, Li_4-V, observed by photoluminescence (PL) at 1045 meV (the ''Q'' center), the carbon-related four-Li center at 1082 meV (S center),[8–10] or the four-Li-related center at 1135 meV (Ref. 8) are examples of this behavior. In those cases the isotope structure of the corresponding zero-phonon line (ZPL) was crucial for revealing the four-Li atom structure of these centers. Similar procedures employing Si with mixed H and D led to the identification of different radiation induced centers involving several hydrogen atoms.[14]

In this work we investigate a different PL center, with its zero-phonon line at 879.3 meV. The results are described as follows. In Sec. III we show that the center is created in the final stages of annealing out radiation-induced point defects in Li-doped silicon. Although it is created at high temperature, the center is unstable at room temperature to passivation by a Li atom. We also show in Sec. III that chemical correlations establish the PL center to contain Li and C atoms, and the presence of Li is confirmed in Sec. VI by isotope doping. We demonstrate in Sec. IV how the intensity of PL from the center depends on temperature, and in particular is quenched at $T > 30$ K with an activation energy of 32 ± 5 meV. Although this value would be consistent with the excited state having a shallow, effective-mass particle, we show in Sec. V that uniaxial stress perturbations establish that the center has tightly bound ground and excited states. The data show that the center has monoclinic I symmetry, with the dipole perpendicular to the defined axis of the center (Sec. V A). For this situation, the relative PL intensities of the stress-split components are not defined by symmetry. In Sec. V B we introduce a simple way of fitting the stress data by using an effective ''s to p'' transition, which accurately describes, in terms of only four parameters, the energies, polarizations and relative intensities of the stress-split components. In Sec. VII we show that the temperature depen-

 ©2000 The American Physical Society

dence of the zero-phonon line can be fitted precisely using a spectrum of coupled phonons that is derived from the vibronic band shape, together with the approximation that the differences in frequencies in the ground and excited electronic states are proportional to the frequency. We begin by describing the experimental methods.

II. EXPERIMENT

Three series of Li-doped silicon crystals have been employed in this work: Czochralski (CZ), 30 Ω cm *p*-type carbon-lean Si; float zone (FZ), 60 Ω cm *n*-type oxygen-lean Si with $[C]=1.6\times10^{17}\,cm^{-3}$, and FZ 1000 Ω cm oxygen- and carbon-lean Si doped with [Li] in the 10^{14}–10^{18}Li cm^{-3} concentration range. Lithium doping was accomplished through diffusion from a one-side natural Li coat. In each series, six samples were heated in Ar atmosphere for 30 min at drive-in temperatures of 300, 350, 400, 450, 500, and 550 °C. The samples were slow cooled and dropped in deionized water to remove the excess of Li. After an RCA cleaning, they were heated for another 2 h at 600 °C in Ar gas to produce an even distribution of Li and were rapidly quenched into silicone oil. To prevent surface damage each face was lapped off ~100 μm. The Li concentration was derived from the variation of electrical resistivity measured by the four-point probe, establishing $[Li]=5\times10^{13}$, 5×10^{14}, 4×10^{15}, 2×10^{16}, 3.5×10^{16}, and $1.1\times10^{17}\,cm^{-3}$. For uniaxial stress measurements we used FZ 60 Ω cm *n*-type oxygen-lean Si with $[C]=1.6\times10^{17}\,cm^{-3}$ and $[Li]=1.1\times10^{17}\,cm^{-3}$. We employed four parallelepiped single crystals of $2\times2\times18\,mm^3$ oriented along $\langle100\rangle$, $\langle111\rangle$, and two along $\langle110\rangle$ for exploring the PL polarization with stress along $\langle110\rangle$ and viewing along either the $\langle1\bar{1}0\rangle$ or the $\langle001\rangle$ directions. The isotope structure was investigated with different ^{6}Li:^{7}Li ratios using the same Li-doped Si crystal series employed elsewhere.[9] The crystals were neutron irradiated at room temperature with a dose of $1\times10^{17}\,cm^{-2}$ 1-MeV equivalent and then annealed during 30–60 min at 550–650 °C. Those samples treated to form the 879.3-meV PL center were stored at $T=77$ K, in order to prevent center destruction upon prolonged room-temperature annealing. Photoluminescence spectra were obtained using Nicolet 60XS or Bomem DA3 fourier transform spectrometers fitted with North Coast Ge diode detectors. Most of the experiments were done with samples immersed in liquid helium at 4.2 K, except for stress experiments and temperature dependence studies that were performed in an Oxford helium flow cryostat. The excitation was accomplished by a 514-nm argon laser operating at 200 mW.

III. CENTER FORMATION, DESTRUCTION, AND PASSIVATION

The effect of neutron irradiation and subsequent annealing at 600 °C of Li-doped Si is shown in Fig. 1(a). As expected for these high annealing temperatures, most of the radiation-induced point defects have been destroyed, and the spectra from FZ Si consist only of two main lines at 879.3 and 1093.2 meV. The latter is an intense feature associated with the emission from an exciton bound to the interstitial Li donor with the creation of one TO phonon.[18,19] This emission

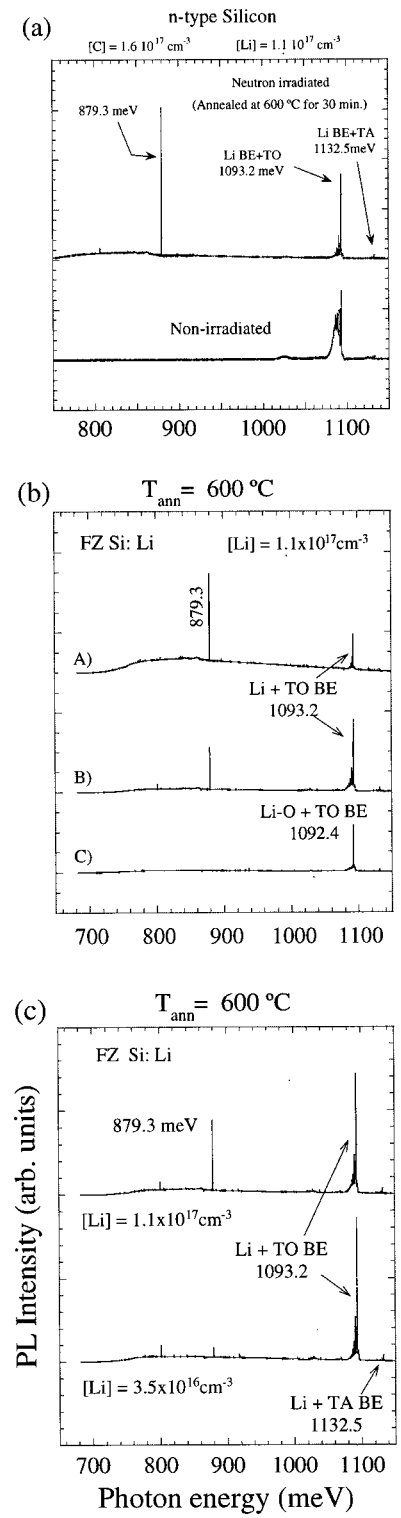

FIG. 1. (a): PL spectra at 4.2 K corresponding to FZ oxygen-lean Si with $[C]=1.6\times10^{17}\,cm^{-3}$ doped with $[Li]=1.1\times10^{17}\,cm^{-3}$, nonirradiated and neutron irradiated with a dose of $1\times10^{17}\,cm^{-2}$ and annealed at 600 °C for 30 min. The neutron-irradiated spectrum evolves to the nonirradiated spectrum upon prolonged room temperature annealing. (b): PL spectra at 4.2 K corresponding to (A) FZ oxygen-lean Si with $[C]=1.6\times10^{17}\,cm^{-3}$, (B) FZ carbon- and oxygen-lean Si and (C) CZ carbon-lean Si doped with $[Li]=1.1\times10^{17}\,cm^{-3}$, neutron irradiated with a dose of $1\times10^{17}\,cm^{-2}$ and annealed at 600 °C for 30 min. (c): Dependence of the PL spectrum of FZ carbon- and oxygen-lean Si on [Li].

is also accompanied by weak multiexciton lines. Bound exciton (BE) luminescence with the emission of one TA phonon is also observable as a minor peak of the PL spectrum at 1132.5 meV. This big difference between the emission intensity for TO and TA is usually found for shallow BE-related luminescence where the vibronic coupling is dominated by silicon TO modes.[12,18,21] Moreover, this Li emission is the unique feature observed in the PL spectrum either from non-irradiated Li-doped FZ Si crystals or from irradiated crystals annealed above about 650 °C [Fig. 1(a)]. Annealing at these temperatures appears to completely remove the effects of radiation damage, and the PL spectrum is very similar to that of the unirradiated crystal.

The strong dependence of the intensity of the 879.3 meV on the Li concentration is illustrated in Fig. 1(b), in samples given our standard treatment of annealing for 30 min at 600 °C. We will confirm in Sec. VI that the center does involve Li. The corresponding effects of varying the carbon and oxygen concentrations are shown in Fig. 1(c). In neutron-irradiated oxygen-lean FZ Si, the PL spectra at 4.2 K is significantly (but not proportionally) larger in material of high carbon ($[C]=1.6\times10^{17}\,cm^{-3}$ compared to $5\times10^{15}\,cm^{-3}$), while in CZ ($[O]=1.4\times10^{18}\,cm^{-3}$) carbon-lean ($[C]<10^{16}\,cm^{-3}$) Si doped with $[Li]=1.1\times10^{17}\,cm^{-3}$ the 879.3 meV line is almost undetectable. Detailed studies confirm that the 879.3-meV ZPL shows its maximum intensity in carbon-enriched crystals, for a given Li concentration. In contrast the effect of oxygen is to inhibit the formation of the defect, whether in the CZ Si [Fig. 1(c)] or in C-enriched FZ Si that has been doped with oxygen (not shown here). In CZ Si, we only observe PL associated with Li bound excitons, shifted (by the oxygen content) to 1092.4 meV. These data strongly suggest that the optical center involves Li and C. The strength of the PL from the Li donors in Fig. 1, which completely dominates the PL from free excitons, shows that the samples still contain substantial amounts of interstitial Li after the irradiation and annealing at 600 °C.

Lithium is well known as a passivator of radiation damage in Si, and the 879.3-meV line undergoes a progressive decrease in its PL intensity upon prolonged annealing at room temperature. The spectrum of Fig. 1(a) was obtained from neutron-irradiated FZ Si immediately after annealing at 600 °C. Storage at room temperature destroys the PL, with a decrease by about $\frac{2}{3}$ occurring after 12 h of room-temperature annealing. The same fractional loss occurs after 15 min for annealing at 100 °C. The variation of PL intensity as a function of the annealing time at 17 and 100 °C is shown in Fig. 2. Although we have not investigated this annealing process in detail, the loss of PL intensity observed at those annealing temperatures suggests that it is probable that there are two decay channels involving long-range migration. In fact, the $I(t)$ behavior of Fig. 2 (full curves) can be accounted for on the assumption that the 879.3-meV center is annealed by complexing with one Li. The faster decay is clearly observed at the two annealing temperatures, and probably reflects a rapid diminution of the Li interstitials liberated during the annealing at 600 °C, due to the formation of Li aggregates or defect complexing processes. Both phenomena are evidenced from the PL spectra through the loss of PL intensity with time exhibited by several Li-related BE lines. Accordingly, the rate equations governing the loss of the 879 centers and

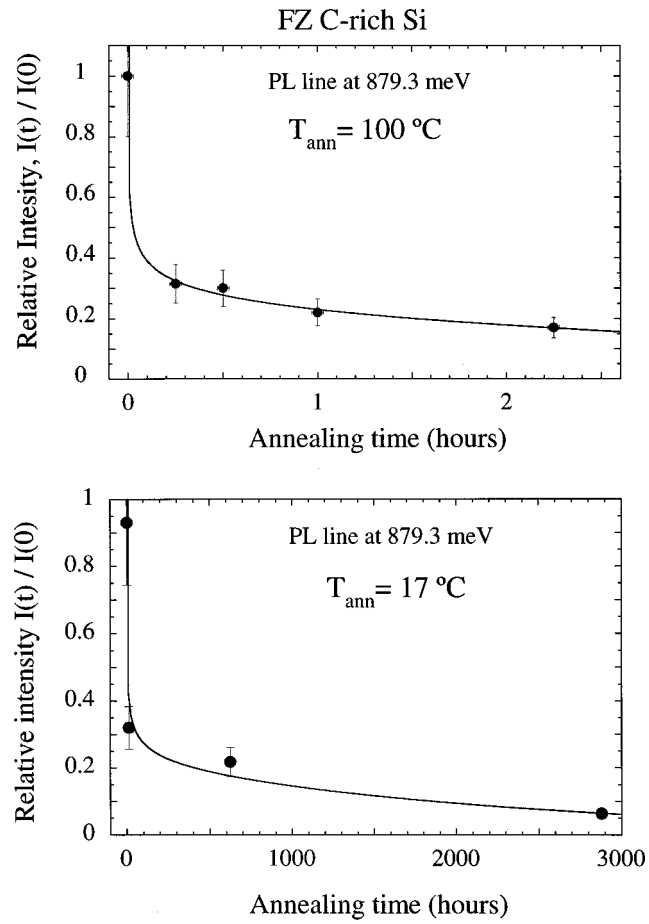

FIG. 2. Dependence of the relative $I(t)/I(0)$ PL intensity at 879.3-meV emission with the annealing time at 17 and 100 °C. Curves represent the least-squares fitting of experimental data to Eq. (2). The fitted lifetime associated with the slower decay, $\tau=\{K[N_{Li}(0)-N_D]\}^{-1}$, is $\tau=5$ and 2350 h at 17 and 100 °C, respectively. The corresponding activation energy is $\Delta E=0.69$ eV.

Li interstitials upon annealing can be written as

$$\frac{dN_{Li}(t)}{dt}=-kN_{Li}(t)\{N_D-[N_0-N_{Li}(t)]\} \quad \text{and}$$

$$\frac{dN_{879}(t)}{dt}=-KN_{Li}(t)N_{879}(t). \tag{1}$$

The first equation relates the loss of Li interstitials, $dN_{Li}(t)/dt$, at time t, where $N_{Li}(t)$ and N_0 are the Li concentration at time 0 and t, respectively, and N_D is an effective concentration of all centers involved in the passivation processes, including Li defects. The difference $N_0-N_{Li}(t)$ represents the concentration of Li-passivated centers at time t. In the present analysis we assume that $N_D\leqslant N_0$. The second equation governs the passivation of the 879 center and depends on the center concentration as well as on the number of Li interstitials. K and k are the appropriate thermally activated rate constants of each process. In particular K is proportional to the Li diffusion coefficient D which depends on the temperature as $D(T)=D_0\exp(-\Delta E/kT)$. By integrating Eqs. (1) we obtain

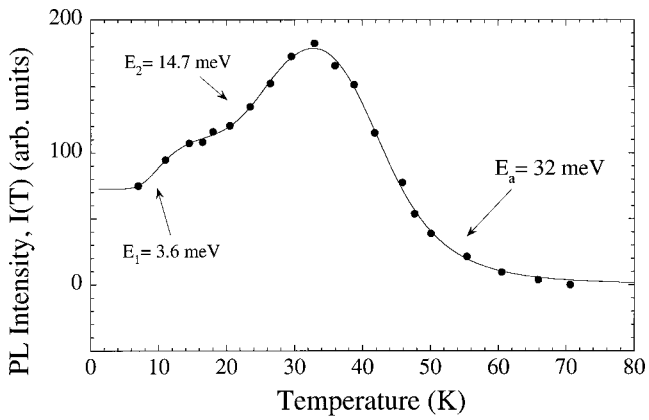

FIG. 3. Variation of the PL intensity at 879.3-meV emission with temperature. The line corresponds to the least-squares fitting of the experimental data to Eq. (3). The three fitted activation energies are indicated.

$$N_{879}(t)=N_{879}(0)\left[\frac{N_0-N_D}{N_0\exp[(N_0-N_D)kt]-N_D}\right]^{K/k}. \quad (2)$$

This equation is represented in Fig. 2 and accounts for the fast and slow decays. We are interested in the limit of long annealing times, as accurate lifetimes can be obtained. For $t\rightarrow\infty$, Eq. (2) becomes

$$N_{879}(t)=N_{879}(0)\left(1-\frac{N_D}{N_0}\right)^{K/k}\exp[-K(N_0-N_D)t].$$

This slower decay has an associated activated energy of 0.69 ± 0.1 eV as derived from the fitted lifetimes, $\tau(T)=[K(N_0-N_D)]^{-1}$, at 290 and 373 K (Fig. 2). The similarity to the diffusion energy of Li (activation energy of 0.66 eV) (Ref. 22) suggests that this annealing-induced reduction of ZPL intensity could be due to the passivation by Li of the center responsible for the 879.3 meV line. In that case the resultant defects would involve at least two Li atoms, and they are evidently not able to produce luminescence in the spectral range explored.

It should be pointed out that the 879.3-meV PL discussed here is not related to PL at 878 meV produced by the ''*W*'' found by Johnson *et al.*[13] upon annealing at 100 °C. The reported annealing temperature for this defect (300 °C) supports this view.

IV. TEMPERATURE DEPENDENCE OF THE PHOTOLUMINESCENCE INTENSITY

Although the 879.3-meV line is a major feature in the $T=4.2$ K PL spectra of FZ *n*-irradiated Si after annealing at 550–600 °C, its intensity increases further with temperature, and reaches a maximum at about 30 K. Figure 3 shows the temperature dependence of the ZPL intensity plus the phonon sideband in FZ Si with $[C]=1.1\times10^{17}\,cm^{-3}$, neutron irradiated to a dose of $1\times10^{17}\,cm^{-2}$ and annealed at 550 °C for 30 min. The PL intensity $I(T)$ increases by a factor 3 from 5 to 30 K, and then progressively decreases and is not detectable above 80 K. There is no luminescence arising from the population of higher-lying excited states to account for the increase of PL intensity. The behavior of $I(T)$ can be explained on the basis of BE emission from an isoelectronic center in competition with exciton trapping and ionization processes involving other centers. The calculated $I(T)$ curve in Fig. 3 describes accurately the experimental intensity and was obtained by assuming that there are two other species of centers competing for exciton capture with the 879.3-meV center. This assumption is based on the double step behavior exhibited by $I(T)$ below the maximum PL intensity temperature, $T=30$ K. The expression for $I(T)$ is then

$$I(T)=\frac{I(0)}{[(1+f_1)(1+f_2)(1+gT^{3/2}\exp(-E_a/kT))]} \quad (3)$$

with

$$f_i=\frac{c_i}{1+g_iT^{3/2}\exp(-E_i/kT)},$$

where E_1 and E_2 are the effective binding energies for excitons at the two species of traps. The f_i parameters represent the fraction of traps that are not ionized and $P=I(0)/[1+gT^{3/2}\exp(-E_a/KT)]$ is the probability of PL, E_a is the binding energy of the exciton at the center and $gT^{3/2}$ is an effective density of states for exciton detrapping.[12] The line of Fig. 3 has been calculated with activation energies of $E_1=3.6$ meV and $E_2=14.7$ meV for exciton ionization from the other centers, and $E_a=32$ meV for the thermal destruction of the PL at 879.3 meV. The uncertainties in these energies are about 30% for the E_1 and E_2, and ±5 meV for the 879.3-meV PL. We identify the shallow trap of $E_1=3.6$ meV with the release of excitons from Li donors for two reasons: (i) the Li exciton binding energy is 3.6 meV,[18,20] and (ii) the first increase of $I(T)$ observed in Fig. 3 correlates with a reduction of the PL intensity associated with the Li at 1093.2 meV (Fig. 1); this PL line is not observed above 20 K. The exciton detrapping by Li donors also correlates with an increase of a broad band PL spreading over a wide energy range below 900 meV, demonstrating the existence of other exciton traps in the sample. The second jump of $I(T)$ is associated with an activation energy of $E_2=14.7$ meV and coincides with the binding energy of the free exciton.[21] The generation of free electrons and holes could ionize competing centers, removing those centers from the exciton capture processes, but given the very few active PL centers in these crystals at $T>30$ K, we do not have independent confirmation of this point. Above about 30 K, the PL intensity decays following a thermal dissociation behavior with an activation energy of 32 ± 5 meV, coinciding with the value expected in Si when one effective mass particle orbits one opposite charge. However, the model of ''pseudodonor'' or ''pseudoacceptor'' in which one of the exciton particles is highly localized to the defect while the other is bound in the Coulomb field of the first, and which applies to many PL centers in Si, does not apply here, for three reasons. We do not observe more shallow excited states by direct observation in the PL spectrum at 30–50 K, nor is there any evidence of them from stress-induced interactions (Sec. V), and third, the splitting of the states under uniaxial stress (Sec. V) is much smaller than expected for an effective-mass hole or electron. Evidently, on trapping, the exciton is better described as two tightly bound particles.

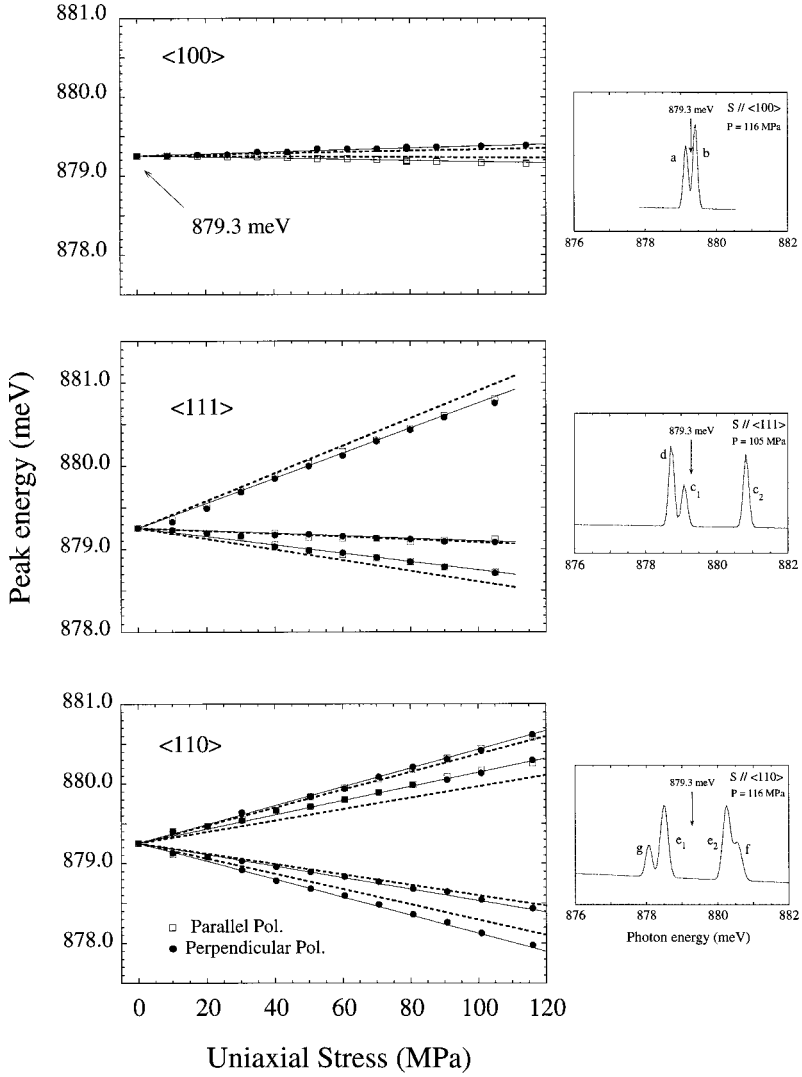

FIG. 4. (Left): Line energy shift versus stress plots. The compression stress is applied along high-symmetry directions in Si. The straight lines represent the experimental shift rate (full line) and the calculated one (dashed line). Energy shifts are given in meV and stress in MPa (see Tables I and II). (Right): Uniaxial stress unpolarized spectra at $T=18$ K of the 879.3-meV line. Peak labeling is included (see Tables I and II).

V. UNIAXIAL STRESS MEASUREMENTS: CENTER SYMMETRY

A. Formal determination of the symmetry

Figure 4 plots the effects on the energy of the 879.3-meV ZPL of compressions along the three high symmetry directions of Si. The spectra recorded with the plane of the PL polarized parallel and perpendicular to the applied stress are given in Fig. 5. We note that there is a linear dependence of the ZPL shifts with the stress (Fig. 4), with no evidence of any stress-induced coupling of excited states and that the intensity of each stress-split component is independent of the stress indicating that the initial states of the stress-split components are not in thermal equilibrium with each other. The observed orientational splitting is consistent with the center's having monoclinic I symmetry.[23] The experimental shift rates and the calculated least-square-fit values with the corresponding A_i parameters ($i=1-4$) for a monoclinic I center are collected in Table I, using the Kaplyanskii notation.[23] In Si, a monoclinic I center has a reflection plane perpendicular to a $\langle 110\rangle$ axis of the crystal.

To confirm the identification, and derive more information about the center, we next analyze the relative PL intensities and polarizations of the stress-split components. In these experiments, the PL is excited by laser light with photon energy ($E_{\mathrm{laser}}=2.4$ eV) greater than the energy gap ($E_{\mathrm{gap}}=1.170$ eV at 4.2 K): the light is absorbed by the silicon crystal and not directly by the optical center. The polarization of the laser beam is lost by the diffusion of excitons to the centers, and all orientations of the monoclinic I centers will be equally excited. Ideally the relative intensities and polarizations of the stress-split components would then be the same in PL as when the 879.3-meV ZPL was measured in absorption (Fig. 6).

The uniaxial stress spectra of Fig. 5 can be explained on the basis of a monoclinic I center having the electric dipole not along the unique $\langle 110\rangle$ axis but in its perpendicular plane. A similar situation was observed for the 488.7-meV carbon-oxygen PL center,[24] where the monoclinic I stress-split pattern displayed by the absorption line could be interpreted as a slightly perturbed orthorhombic center with the electric dipole close to $\langle 001\rangle$ in the (110) plane. In the present case, the polarized spectra of the 879.3 line fit well if we consider that the dipole makes an angle of $-10°$ with $\langle 111\rangle$. Table II collects the observed normalized intensity of each stress-split component. The calculated intensity of each perturbed ZPL component as would be measured in absorption is given in Fig. 6(a) as a function of the angle θ that the electric dipole makes with the $\langle 111\rangle$ direction. For absorp-

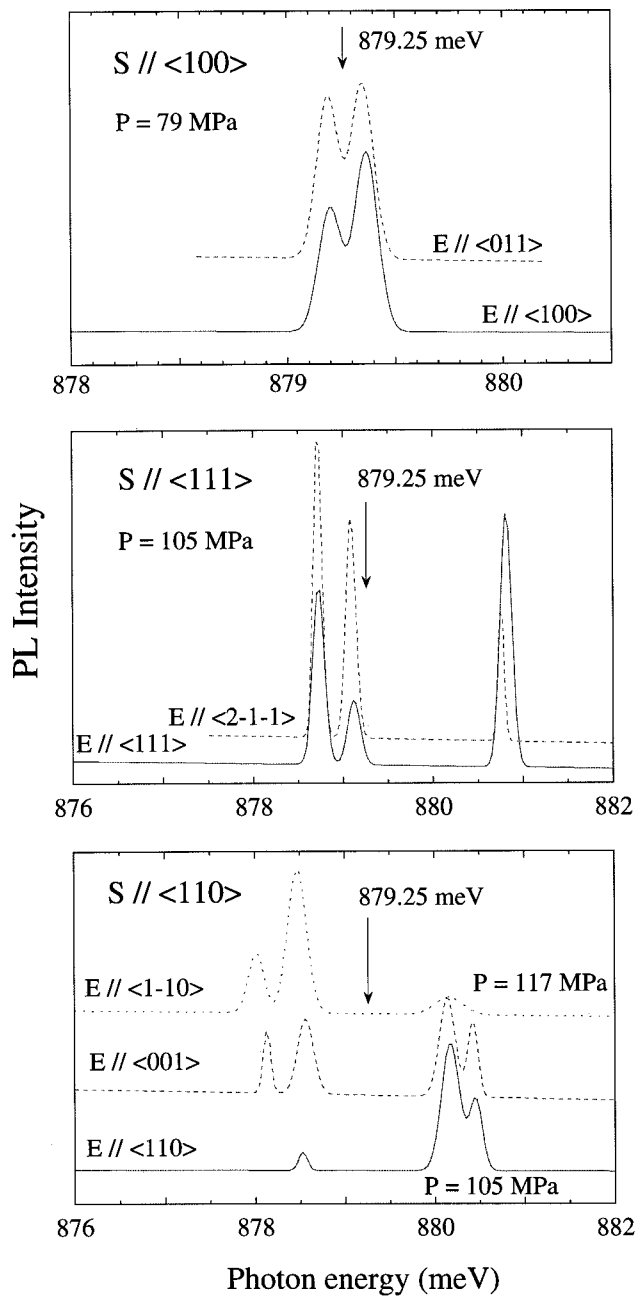

FIG. 5. Polarized spectra at $T=18$ K of the 879.3-meV line, with stress directed along high-symmetry directions, and the electric vector of the PL light parallel and perpendicular to the stress, respectively. Note that for stress along $\langle 110\rangle$, two different perpendicular orientations ($\langle 1\bar{1}0\rangle$ and $\langle 001\rangle$) have been explored. The normalized intensity of each component is given in Table II, and compared with the calculated intensities (Fig. 6).

tion, the intensities have been obtained by evaluating, as a function of θ, the scalar products of the unit vector along the polarizer and the unit vectors along the electric dipoles associated with the 12 symmetry-equivalent centers. In a real PL experiment, this procedure must be modified in order to account for all the PL intensity emitted within the solid angle of detection. The curves of Fig. 6(b) have been calculated by integrating the emitted photons within a solid angle of $\frac{4}{3}$ radians, which is similar to that attained in actual PL experiments. The intensity pattern however is very similar to that for absorption; the intensity difference provided by these methods is, in the extreme case, lower than 10%. Polarization measurements in PL are less accurate than those performed by absorption, not only due to the wide solid angle of emission but also due to depolarization processes by reflection at crystal faces. Nevertheless, there is good agreement between the experimental and calculated intensities for $\theta=-10°$, placing the dipole of the center close to the $\langle 111\rangle$ axis.

B. A simple picture

A simple view of the stress data of Figs. 4 and 5 is to use a descendant symmetry scheme as follows. Consider an $s\rightarrow p$ electric-dipole allowed transition at a center with T_d symmetry. The effects of uniaxial stresses on this transition can be determined by three parameters: A, B, and C.[23] The stress parameters A and B describe the changes in energy of the p_z state unit hydrostatic stress S and a unit S_θ stress, respectively, and C is defined through CS_{xy} being the coupling for the p_x and p_y states by a unit S_{xy} stress. Let us now reduce the symmetry from T_d to monoclinic I(C_{1h}). The reflection plane in C_h must lie along $\langle 110\rangle$ axes; we take the [110] orientation as the primary orientation of the center. The combination $\Psi=\alpha(p_x-p_y)+\beta p_z$, with $2\alpha^2+\beta^2=1$ gives a state with a dipole moment at an angle $\cos^{-1}(\beta)$ to the [001] axis and perpendicular to [110]. The stress perturbation $\langle\Psi V\Psi\rangle$, where V is the general stress operator, of the state Ψ can be written in terms of the parameters A, B, C as

$$\langle\Psi V\Psi\rangle=[A-2B(\alpha^2-\beta^2)]S_{zz}+[A+B(\alpha^2-\beta^2)]\times(S_{xx}+S_{yy})-2\alpha^2CS_{xy}+2\alpha\beta C(S_{xz}-S_{yz}), \tag{4}$$

where the S_{ij} are the stress-tensor components defined in terms of the crystal's Cartesian axes. In terms of the Kaplyanskii's notation for a monoclinic I center,[23] the stress parameters are given by

$$A_1^m=A-2B(\alpha^2-\beta^2);\quad A_2^m=A+B(\alpha^2-\beta^2);$$
$$A_3^m=-\alpha^2C;\quad A_4^m=\alpha\beta C. \tag{5}$$

Note that for trigonal symmetry with electric dipole along $[1\bar{1}\bar{1}]$ $\alpha=-\beta=1/\sqrt{3}$, and so

$$A_1^m=A_2^m=A_1^t \text{ and } A_3^m=A_4^m=A_2^t.$$

The monoclinic I theory accounts for the observed shift rates. A least-squares fit to the stress-induced perturbations to the energies gives the four parameters A, B, C, and β as $A=0.48$ meV/GPa, $B=1.43$ meV/GPa, $C=25.17$ meV/GPa, and $\beta=0.41$, predicting shift rates of 0.8 and -0.2 along $\langle 100\rangle$; 16.5, -1.7, and -6.4 along $\langle 111\rangle$; and 11.2, 7.2, -6.6, and -9.5 along $\langle 110\rangle$, all in meV/GPa units. These shifts approximate the measured rates (Table I). The value of $\beta=0.41$ implies that the dipole is at an angle $\phi=\cos^{-1}\beta=65.8°$ with [001]. Considering the trigonal angle of 54.7°, the dipole is making an angle of $-10°$ with the [111] (bond direction) axis (i.e., $\theta=170°$ in the intensity diagrams of Fig. 6). As we have seen in Sec. III A, this value

TABLE I. Stress data for the 879.3-meV line. The experimental shift rates and the calculated ones (in parentheses) from least-squares fitting to the theoretical expressions for monoclinic I symmetry given in the second column are in meV/GPa units. Fit parameters: $A_1=-0.20$; $A_2=0.82$; $A_3=-10.38$; $A_4=6.82$ (meV/GPa); (see text) $A=0.48$; $B=1.43$; $C=25.17$ (meV/GPa); $\alpha=0.64$ and $\beta=0.41$.

Direction stress	Theoretical expressions	Experimental (calculated) shift rates (meV/GPa)
⟨100⟩	$a=A_1$	−0.8 (−0.2)
	$b=A_2$	1.2 (0.8)
⟨111⟩	$c_2=(A_1+2A_2-2A_3+4A_4)/3$	15.0 (16.5)
	$c_1=(A_1+2A_2-2A_3-4A_4)/3$	−1.7 (−1.7)
	$d=(A_1+2A_2+2A_3)/3$	−5.1 (−6.4)
⟨110⟩	$f=A_2-A_3$	11.8 (11.2)
	$e_2=(A_1+A_2+2A_4)/2$	8.9 (7.2)
	$e_1=(A_1+A_2-2A_4)/2$	−6.8 (−6.6)
	$g=A_2+A_3$	−11.0 (−9.5)

of β provides also the best fit to the observed polarization intensities of Fig. 5 thus confirming the present interpretation.

The direction of the dipole moment predicted by this model is close to the bonding direction of nearest neighbors in Si. The quasitrigonal symmetry of this center is confirmed by noting that the splitting pattern is similar to that expected for a transition between nondegenerate orbital states in a center of trigonal symmetry, for which there is no splitting for stresses along ⟨100⟩ and there are two stress-split components along ⟨111⟩ and ⟨110⟩. Indeed, the gross features of the splitting may be described using the two parameters for a trigonal center ($A_1^t=0.48$ and $A_2^t=8.39$ meV/GPa in Kaplyanskii's notation).

In conclusion, the 879.3-meV PL center has monoclinic I symmetry with the dipole lying in the reflection plane, close to the ⟨111⟩ axis; it can be described as a slightly perturbed trigonal center, and the shift rates and relative intensities are also understandable using only four parameters starting from a T_d center. Compared to the splitting of the conduction-band minima (by 92.5 meV/GPa for ⟨001⟩ stress[25]) and the valence-band maxima (by 45 ± 2 meV/GPa for ⟨001⟩ stress[25]), the effects on the 879.3-meV line are very small, confirming that the transition involves highly localized electronic states at the center.

VI. CHEMICAL NATURE OF THE CENTER

Figure 7(a) shows a high-resolution spectrum of the ZPL measured in a sample doped with natural Li. Two structured components can be seen at 879.07 meV (a weak component) and at 879.25 meV (a strong component). The measured integrated intensity for these components, 0.07:0.93, is very similar to the natural isotope abundance of ^{6}Li:^{7}Li, suggesting that the ZPL is perturbed by the effects of one Li atom. This result is confirmed by the isotopic structure displayed by the present ZPL in crystals doped with different ^{6}Li:^{7}Li isotopic ratios [Fig. 7(b)]. A ZPL at 879.1 meV is obtained in ^{6}Li-enriched FZ Si, while for an isotope ratio of 0.54:0.46 the components could not be clearly resolved spectroscopically but, as expected, the envelope is centered at about 879.2 meV. The center therefore contains at least one Li atom. The isotopic shift, $\Delta E=E(^7\mathrm{Li})-E(^6\mathrm{Li})=0.18$ meV, is similar, per active Li atom, to that observed for the Q center (Li_4-V) (Ref. 11) and the four-Li center[8] recently identified in irradiated silicon.

The presence of C can be inferred from the dependence of the ZPL intensity on the C concentration in the two FZ Si crystals investigated (Fig. 1). Efforts to form this center in mixed ^{12}C- and ^{13}C-doped FZ Si for isotope analysis were unsuccessful due to incorporation of oxygen from quartz during the in-diffusion of ^{13}C (carried out with methane at 1300 °C for 7 days). The presence of oxygen in the crystal was revealed by a prominent C line (789.6 meV) observed in PL whose intensity was an order of magnitude higher than the intensity of the G line (969.4 meV) in FZ Si with [C] $=1.6\times10^{17}$ cm^{-3}. This figure is contrary to that expected for neutron-irradiated C-rich and O-lean crystals whose PL spectrum is dominated by the two-carbon G line.[8] This unintentional doping with oxygen during the ^{13}C in-diffusion processes inhibited the formation of the center being investigated here and therefore no conclusive result about its carbon structure could be obtained from isotope experiments.

In addition to the dependence of the ZPL intensity with [C] and following the discussion given in Ref. 24, we also note that the stress parameters A_i are similar in magnitude to those obtained for radiation damage centers involving C interstitials trapped at another impurities[26,27] and smaller, for example, than those associated with a vacancy cluster.[28] Therefore the presence of at least one C interstitial in the present center is likely. Examination of the vibronic side band, in the next section, supports this conclusion.

VII. VIBRONIC PROPERTIES

A. Phonon sideband and coupled modes

Figure 8 shows the vibronic sideband associated with the ZPL at 879.3 meV. It can be seen that the phonon spectrum is dominated by resonant phonons having vibrational energies close to the acoustical transverse mode energy in pure Si. The one-phonon spectrum consists mainly of phonons at 16 meV and less-strongly coupled modes at 31 and 36 meV. The comparison between the temperature dependence of the ZPL intensity and the 66.3-meV peak intensity in the 5–70-K range, allows us to identify the peak at 66.3 meV as

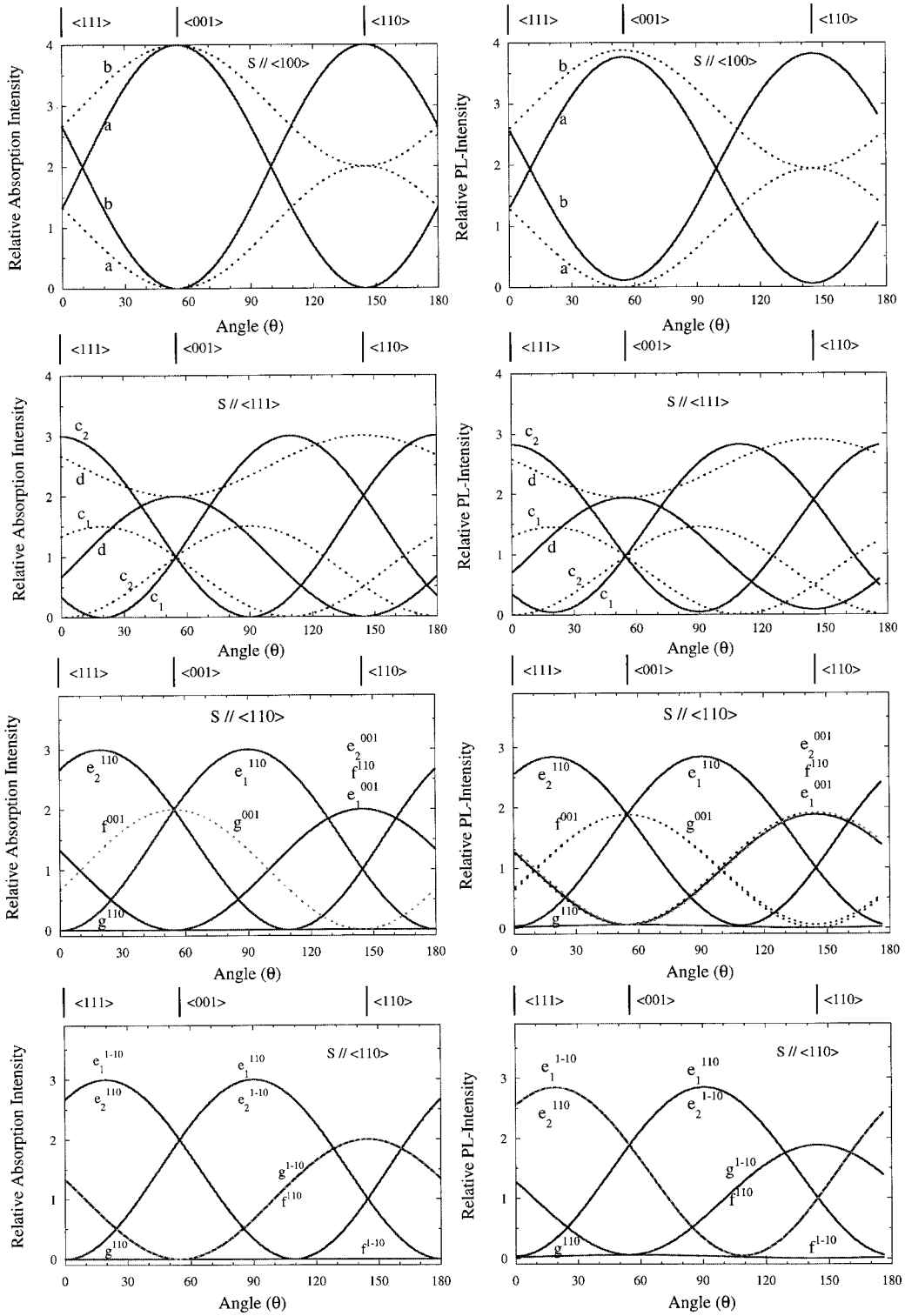

FIG. 6. Calculated intensity of the stress split components of a monoclinic I center with the transition dipole in the (110) plane. θ is the angle formed by the dipole and the [111] direction. $I(\theta)$ has been calculated for stress applied along high-symmetry directions in silicon: ⟨100⟩ (components a and b), ⟨111⟩ (components c_1, c_2, and d) and ⟨110⟩ (components e_1, e_2, f, and g). The curves on the left side correspond to components calculated for absorption while curves on the right side correspond to PL. In the latter case, the intensity has been calculated by integrating the emitted intensity polarized parallel to the stress and perpendicular to it within a solid angle of $\frac{4}{3}$ rad.

a local mode (LM) of this center. The possibility that this peak could correspond to a ZPL from another center is definitively ruled out as both intensities (ZPL and LM) exhibit the same intensity variation and anneal at the same temperature. The presence of a LM with this energy is noteworthy since most of the observed LM modes with energies around 66 meV correspond to *C* interstitial centers[12] thus supporting the suggestion that interstitial carbon is involved in the center. In particular, LM with this energy have been detected in the C- and O-related PL centers at 488 meV (64.5 meV),[24] at

TABLE II. Relative polarized intensity of the 879.3-meV PL line. The experimental polarized intensity of each stress-perturbed ZPL is given for polarization with E parallel to the stress direction and perpendicular to it for three high-symmetry stress directions. The corresponding calculated intensities for absorption and PL (see text), respectively, are given in parentheses. PL intensity has been calculated on the assumption that the transition dipole is in the reflection (011) plane, and makes an angle of $-10°$ ($\theta=170°$) with the C_3 $\langle 111\rangle$ axis. Note that for the $\langle 110\rangle$ stress, we obtained two different polarizations perpendicular to the stress direction: $\langle 001\rangle$ and $\langle 1\bar{1}0\rangle$.

Direction stress	ZP lines Experimental (calculated) polarized intensity			
$\langle 100\rangle$	a		b	
$pol \parallel P(100\rangle$	1.6 (0.8, 0.8)		2.4 (3.1, 3.0)	
$pol \parallel \langle 011\rangle$	1.9 (1.6, 1.5)		2.1 (2.4, 2.3)	
$\langle 111\rangle$	c_2	c_1		d
$pol \parallel \langle 111\rangle$	2.1 (2.9, 2.8)	0.5 (0.5, 0.7)		1.4 (0.5, 0.5)
$pol \parallel \langle 2\bar{1}\bar{1}\rangle$	0.5 (0, 0)	1.6 (1.2, 1.3)		1.9 (2.8, 2.7)
$\langle 110\rangle$	f	e_2	e_1	g
$pol \parallel \langle 110\rangle$	1.2 (1.6, 1.5)	2.4 (2.3, 2.3)	0.4 (0.0, 0.1)	0.0 (0.0, 0.0)
$pol \parallel P(001\rangle$	0.5 (0.4, 0.4)	1.6 (1.6, 1.6)	1.2 (1.6, 1.6)	0.7 (0.4, 0.4)
$pol \parallel \langle 1\bar{1}0\rangle$	0.0 (0.0, 0.0)	0.4 (0.1, 0.1)	2.7 (2.3, 2.4)	0.9 (1.6, 1.5)

767 meV (the P center; 65.6 meV),[29,30] and at 789 meV (the C center; 65.5 meV).[30,31] They are also observed in the carbon center at 969 meV (the G center) and its variants,[27] and at the hydrogen- and carbon-related at 935 meV (the T center; 66.3 meV).[32–34] In each case carbon is involved as an interstitial species.

The vibronic sideband associated with the 879.3-meV ZPL can be well reproduced from the one-phonon spectrum $I_1(\omega)$, shown in Fig. 8(a). The one-phonon spectrum $I_1(\omega)$ is normalized to 1: $\int_0^\infty I_1(\omega)d\omega=1$. The complete vibronic side band was obtained from $I_1(\omega)$ by evaluating the n-phonon contribution $P_n(\omega)$ to the vibronic band as $I_{\mathrm{PL}}^{\mathrm{VIB}}(\omega)=\Sigma_1^\infty P_n(\omega)$ where $I_{\mathrm{PL}}^{\mathrm{VIB}}(\omega)$ is the corrected experimental vibronic band[12,35] associated with the ZPL and $P_n(\omega)$ is defined as

$$P_n(\omega)=\int_0^\infty P_{n-1}(\omega-x)P_1(x)dx,$$

where $P_1(\omega)=I_1(\omega)S\exp(-S)$ and $P_n(\omega)$ satisfies the integral condition

$$\int_0^\infty P_n(\omega)d\omega=\exp(-S)\frac{S^n}{n!} \tag{6}$$

The points of Fig. 8(b) have been calculated using this method with a Huang-Rhys factor $S=1.1$. Interestingly, the one-phonon spectrum is, as for many of the PL centers in silicon,[12] dominated by a prominent resonance at 16 meV which is probably associated with TA phonons near the zone boundary in the [100] direction. Other resonant modes at 31 and 36 meV are also significantly coupled to the BE. There is no appreciable contribution from Si phonons associated with a maximum in the phonon density, therefore suggesting that the electronic states are probably highly localized at the center. In the simplest one-coordinate model Q, we can estimate an effective electron-phonon coupling c from the Huang-Rhys factor through the expression[12] $S=c^2/2m\hbar\omega^3$. Taking the Si atomic mass as the more appropriate when lattice modes are involved in the phonon sideband, and the mean phonon energy obtained from $I_1(\omega)$, $\hbar\omega=23$ meV, we obtain $c=456$ meV Å^{-1}. This value must be compared with the coupling parameters C_{XX}, C_{YY}, C_{ZZ}, and C_{XY}, where X, Y, and Z refer to the *local* axes of the center. These axes are defined, for the [110]-oriented center of Sec. V B, as $X=[1\bar{1}2]$, $Y=[1\bar{1}\bar{1}]$, and $Z=[110]$. The coupling parameters associated with modes producing each deformation can be obtained easily from uniaxial stress data:

$$C_{XX}=(A_1c_{11}+2A_2c_{12})/1=31.2\ \mathrm{meV\ Å^{-1}},$$

$$C_{YY}=[A_1c_{12}+A_2(c_{11}+c_{12})-A_3c_{44}]/1=431\ \mathrm{meV\ Å^{-1}},$$

$$C_{ZZ}=[A_1c_{12}+A_2(c_{11}+c_{12})+A_3c_{44}]/1=-279\ \mathrm{meV\ Å^{-1}},$$

$$C_{XY}=A_4c_{44}/1=233\ \mathrm{meV\ Å^{-1}}. \tag{7}$$

In these calculations, we used the elastic constants of Si (Ref. 36) thus assuming that they are unchanged near the optical center, the stress parameters given in Table I and the characteristic Si-Si interatomic distance, $1=2.34$ Å.[12] As expected from stress data of Fig. 4, those modes associated with atomic motions approximately along the dipole direction, i.e., near $\langle 111\rangle$, provide the highest electron-phonon coupling. The large ZPL splitting observed for stress parallel to $\langle 111\rangle$ reflects this phenomenon. In contrast to this, the small ZPL shift along $\langle 100\rangle$ demonstrates that a hydrostatic deformation does not contribute significantly to the phonon band. Given that the Huang-Rhys factor depends on the square of the C_{ij}, the coupling from the biggest term, C_{YY}, will dominate in the vibronic coupling. In fact, the Huang-Rhys factor deduced from the C_{YY} coupling constant is $S=1.12$ and satisfactorily reproduces the experimental value.

B. The zero-phonon line

Figure 9 shows the variation of the width $W(T)$, energy $E(T)$, and Huang-Rhys factor $S(T)$ of the 879.3-meV ZPL

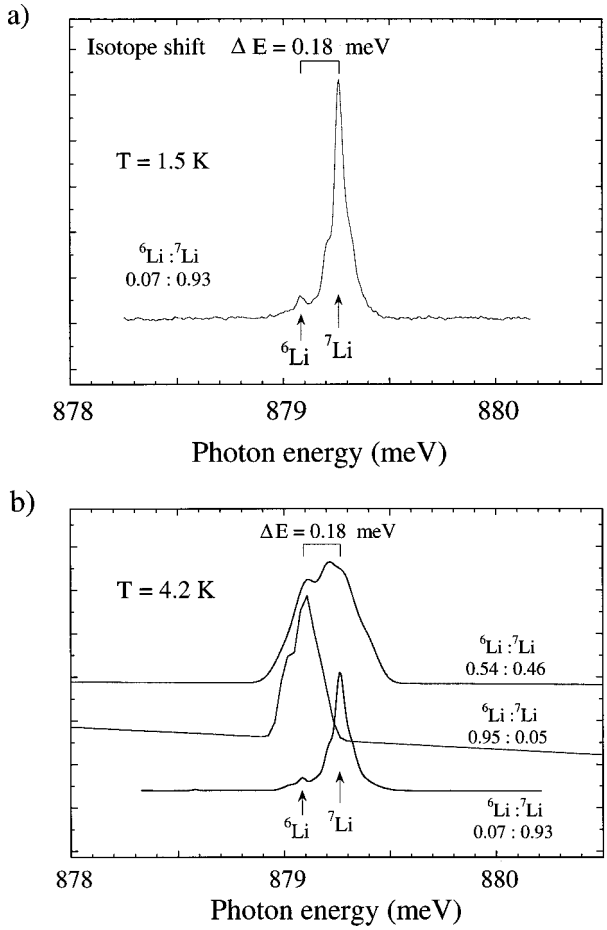

FIG. 7. (a): High-resolution spectrum of the 879.3-meV ZPL at 1.5 K obtained in FZ oxygen-lean Si with $[C]=1.6\times10^{17}\,cm^{-3}$ and with natural Li ($[Li]=1.1\times10^{17}\,cm^{-3}$), neutron irradiated and annealed at 600 °C for 30 min. Spectral resolution: 0.012 meV. The same spectrum is obtained at 4.2 K. The two Li isotope components and the corresponding shift are indicated. The measured relative intensity of each component is 0.07 (^{6}Li) and 0.93 (^{7}Li), and coincides the natural abundance of the respective isotopes. (b): PL spectra showing the Li-isotope effect on the 879.3-meV ZPL. The spectra correspond to different neutron-irradiated FZ C-enriched Si crystals doped with different ^{6}Li:^{7}Li concentrations and annealed at 550–600° at 30 min. The ^{6}Li:^{7}Li concentrations are: 0.07:0.93 (natural lithium); 0.54:0.46 and 0.95:0.05. The spectral resolutions are 0.024 meV for the 007:0.93 crystal and 0.06 meV for the double Li-doped 0.54:0.46 and 0.95:0.05 crystals.

with temperature in the 5–70-K range. Interestingly, the observed variation provides precise information about the electron-phonon coupling governing the thermal shift and the thermal broadening of the ZPL, i.e., the phonon energy difference $\Delta\omega$ between the ground and excited electronic states which we will show can be taken to be simply $\Delta\omega=\alpha\omega^n$. In addition, the investigated PL center is a clear example of large thermal redshift dominated by this phonon term (usually named the explicit contribution): $(\partial E/\partial T)_{\rm vol}$. In contrast, the contribution due to thermal expansion effects (implicit contribution) is smaller than 1% of the phonon contribution:

$$(\partial E/\partial V)_T(\partial V/\partial T)_P<0.01(\partial E/\partial T)_{\rm Vol}.$$

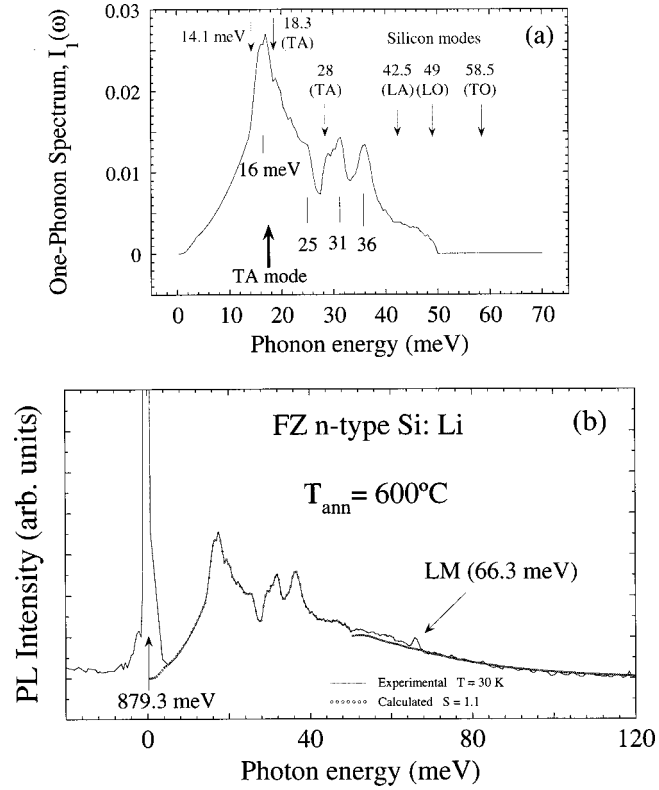

FIG. 8. (a) Normalized one-phonon spectrum $I_1(\omega)$: $\int_0^\infty I_1(\omega)d\omega=1$, associated with the vibronic band of the 879.3-meV ZPL. The phonon energies at top correspond to phonon energy at maximum phonon density, whereas the energies at bottom correspond to resonant modes coupled to bound exciton in the 879.3-meV center. Note that transverse acoustical (TA) resonant modes provide the strongest electron-phonon coupling. (b): Phonon spectrum of the 879.3-meV line at 18 K. Resolution: 1.2 meV. The points represent the calculated phonon sideband from the one-phonon spectrum shown in (a) using a Huang-Rhys factor of 1.1. The small peak at 66.3 meV is a local mode.

This behavior could be anticipated by the small values of A_1 and A_2 (Table I), since (A_1+2A_2) is the rate of change of transition energy under hydrostatic pressure. For comparison purposes, note that the lattice contraction of Si from 0 to 60 K is $\Delta a/a=-1.0\times10^{-5}$, so that the associated expansion shift is

$$\delta_{\rm IM}=-(A_1+2A_2)(c_{11}+2c_{12})\frac{\Delta a}{a}=0.004\ \text{meV}, \quad (8)$$

much smaller than the experimental shift of -0.52 meV found for this center [Fig. 9(a)]. The total shift is therefore completely dominated by the phonon term.

The variations of $S(T)$, $E(T)$, and $W(T)$ shown in Fig. 9 can be explained on the basis of the one-phonon spectrum $I_1(\omega)$, deduced from the analysis of the vibronic sideband [Fig. 8(b)]. The integral expressions for $E(T)$, $W(T)$, and $S(T)$ (Refs. 12 and 35–39) employed here to simulate the observed variations and the corresponding fitting parameters are, respectively,

$$E_{\rm ZPL}(T)=E_{\rm ZPL}(0)+\delta_{\rm EX}(T)+\delta_{\rm IM}(T) \quad (9)$$

with

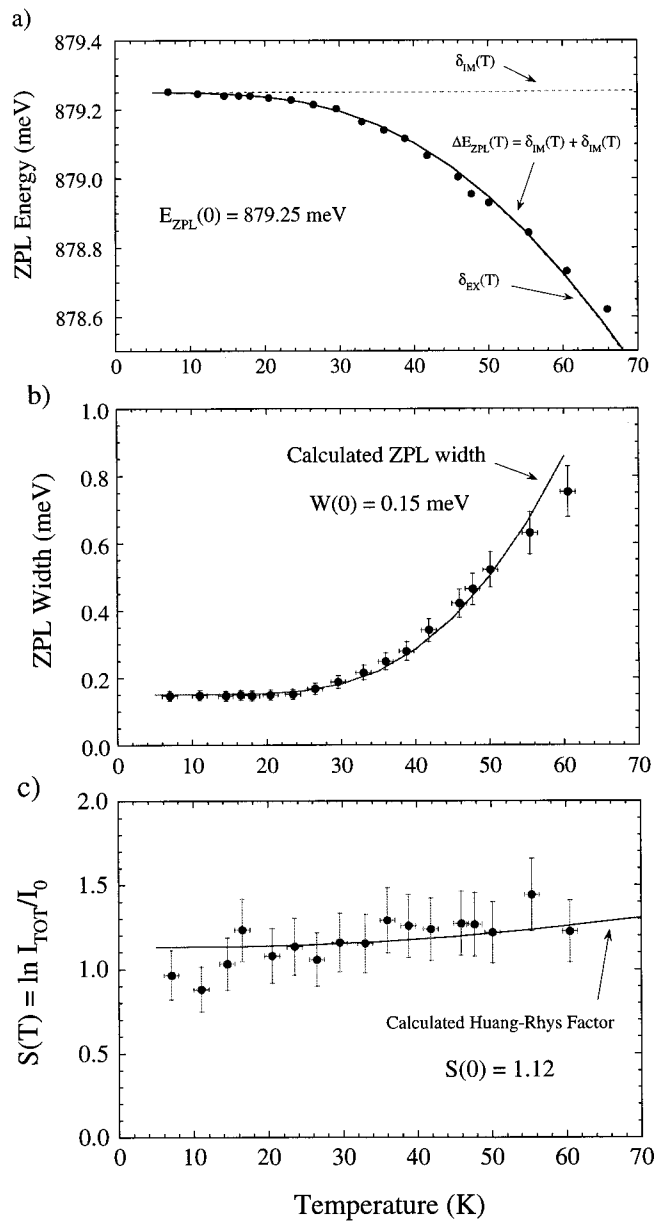

FIG. 9. Variation of different spectroscopic parameters of the 879.3-meV PL center with temperature: (a) ZPL energy, (b) ZPL width, and (c) the Huang-Rhys parameter $S(T)$, defined as the logarithm of the ZPL intensity to the total PL intensity ratio. The curves represent the calculated variations using the one-phonon spectrum of Fig. 8(a). The analytic expressions (Refs. 35 and 37) and the fitted parameters are given through Eqs. (8)–(13).

$$\delta_{\mathrm{IM}}(T) = -(A_1 + 2A_2)\left(\frac{c_{11} + 2c_{12}}{3}\right)\frac{\Delta V}{V}(T) \tag{10}$$

and

$$\delta_{\mathrm{EX}}(T) = \alpha \int \omega I_1(\omega) n(\omega, T) d\omega \tag{11}$$

with $\alpha = -0.95$ (in meV units),

$$W(T) = W(0) + b \int [0.95 \omega I_1(\omega)]^2 n(\omega, T)[1 + n(\omega, T)] d\omega \tag{12}$$

with $b = 6.1$ and $W(0) = 0.15$ (in meV units), and

$$S(T) = S(0) \int_0^{\omega_M} I_1(\omega)[1 + 2n(\omega, T)] d\omega, \tag{13}$$

where $n(\omega, T)$ is the Bose-Einstein occupancy factor given by $n(\omega, T) = [\exp(-\hbar\omega/kT) - 1]^{-1}$.

The results of these calculations are shown in Fig. 9.

Several important facts can be drawn from this analysis: (i) the functions $E(T)$ and $W(T)$ are very sensitive to the form of the electron-phonon coupling. If we write the change in phonon frequency between the ground and excited electronic states as $\Delta\omega = \alpha\omega^n$, an exponent $n = 1$ reproduces the experimental variations more accurately than exponent values $n > 1$. The best variation for $E(T)$ is found for $\alpha = -0.95$ (meV units), which implies a zero point energy shift of the ZPL:

$$\tfrac{1}{2} \int_0^{\infty} \alpha \omega I_1(\omega) d\omega = -11\,\mathrm{meV}.$$

The negative sign indicates that the phonon energies in the excited state are lower than in the ground, as usually found for Si centers. This leads to thermal redshifts of ZPL upon increasing temperature as has been observed in most cases where the phonon contribution is dominant.

(ii) The variation of the ZPL width $W(T)$ is also well reproduced through the functional $g(\omega) = \alpha\omega I_1(\omega)$, with a fit model parameter $b = 6.1$ [Fig. 9(b)], which is close to the expected value $b = 2\pi$.[35,37] (iii) The thermal expansion contribution to the ZPL shift is much lower than the phonon contribution due to different value of the phonon energy in the ground and excited electronic states. As Fig. 9(a) shows, the shift of -0.52 meV experienced by ZPL from 5 to 60 K is actually due to the phonon contribution, whose contribution $\delta_{\mathrm{EX}}(60) = -0.53$ meV is much higher than the implicit one $\delta_{\mathrm{IM}}(60) = +0.004$ meV. This behavior contrasts with findings in localized centers like those attained in transition metal complexes such as, for example, $MnF_6{}^{4-}$ systems, where the implicit contribution to the thermal shift for crystal field peaks is found to be about 40% of the total thermal shift.[38,39]

VIII. CONCLUSIONS

In conclusion, the present analysis indicates that the center is monoclinic I (quasitrigonal) with the electric dipole within the (110) plane and at $-10°$ from [111]. Based on this fact, the high annealing temperatures required to form the center, the need for C in the lattice, the evidence for (at least) one Li atom, the efficient thermal passivation of the center at room temperature, and the existence of a LM of 66.3 meV, a possible model for this center is a carbon radiation damage involving a Li atom, perhaps as an analog of the hydrogen-carbon centers like the T center.[32–34] If so, one can anticipate a family of Li-related centers parallel to the H-related centers; however, more research is needed to substantiate this suggestion. The investigated center is a model example for which the electron-phonon coupling can be described by changes in the vibrational frequencies as $\Delta\omega = \alpha\omega$ for all coupled modes. The ZPL thermal shift is fully dominated by

the explicit contribution while the thermal-expansion effects are negligible. The Huang-Rhys factor characterizing the phonon sideband is mainly governed by those modes providing atomic displacements nearly along the electric dipole direction ⟨111⟩. Finally, the high exciton binding energy ($1145.5-879.3=266.2$ meV) and the uniaxial stress shifts firmly suggest that the PL is associated with an isoelectronic deep center with the two excitonic particles tightly bound at the center.

ACKNOWLEDGMENTS

Thanks are due to Dr. A. Safonov for fruitful discussions. One of us (F.R.) is indebted to the DGICYT (Grant Ref. PR95-282) for financial support. F.R. also thanks the Solid State Group at King's College, London, for the hospitality and friendship extended to him during his sabbatical. This work was financed by the Engineering and Physical Science Research Council.

*Author to whom correspondence should be addressed. Present address: DCITIMAC, Facultad de Ciencias, University of Cantabria, 39005 Santander, Spain. Email address: rodriguf@unican.es

[1] E. Ö. Sveinbjörnsson, S. Kristjansson, and H. P. Gislason, J. Appl. Phys. **77**, 3146 (1995).
[2] H. P. Gislason, S. Kristjansson, and E. Ö. Sveinbjörnsson, Mater. Sci. Forum **196**, 695 (1995).
[3] L. T. Canham, Ph.D. thesis, University of London, 1983.
[4] U. Wahl, M. Restle, C. Ronning, H. Hofsäss, and S. G. Jahn, Phys. Rev. B **50**, 2176 (1994).
[5] T. K. Kwok, J. Lumin. **65**, 327 (1995).
[6] P. Alteheld, S. Greulich-Weber, J. M. Spaeth, H. Weihrich, H. Overhof, and M. Hohne, Phys. Rev. B **52**, 4998 (1995).
[7] H. Weihrich, H. Overhof, P. Alteheld, S. Greulich-Weber, and J. M. Spaeth, Phys. Rev. B **52**, 5007 (1995).
[8] F. Rodríguez, G. Davies, and E. C. Lightowlers, Mater. Sci. Forum **258-263**, 411 (1997).
[9] F. Rodríguez, G. Davies, and E. C. Lightowlers, Mater. Sci. Forum **258-263**, 635 (1997).
[10] G. Davies, L. T. Canham, and E. C. Lightowlers, J. Phys. C **17**, L173 (1984).
[11] E. C. Lightowlers, L. T. Canham, G. Davies, M. L. W. Thewalt, and S. P. Watkins, Phys. Rev. B **29**, 4517 (1984).
[12] G. Davies, Phys. Rep. **176**, 83 (1989), and references therein.
[13] E. S. Johnson, W. D. Compton, J. R. Noonan, and B. G. Streetman, J. Appl. Phys. **44**, 5411 (1973).
[14] A. N. Safonov and E. C. Lightowlers, Mater. Sci. Eng., B **36**, 251 (1996).
[15] G. Davies and M. H. Nazaré, *Proceedings of the 19th International Conference on Defects in Semiconductors* (Trans Tech Publications, Aveiro, 1997), pp. 171–340.
[16] S. J. Pearton, J. W. Corbett, and M. Stavola, *Hydrogen in Crystalline Semiconductors* (Springer-Verlag, Berlin, 1992).
[17] E. C. Lightowlers and G. Davies, *Proceedings of the NATO Conference on Early Stages of Oxygen Precipitation in Silicon, Exeter, 1996* (Kluwer Academic Publishers, The Netherlands, 1996).
[18] M. L. W. Thewalt, Solid State Commun. **28**, 361 (1978).
[19] M. O. Henry and E. C. Lightowlers, J. Phys. C **13**, 2215 (1980).
[20] S. A. Lyon, D. L. Smith, and T. C. McGill, Solid State Commun. **28**, 317 (1978).
[21] K. L. Shaklee and R. E. Nahory, Phys. Rev. Lett. **24**, 942 (1970).
[22] C. S. Fuller and H. Reiss, J. Chem. Phys. **27**, 358 (1957).
[23] A. A. Kaplyanskii, Opt. Spectrosc. **16**, 329 (1964).
[24] G. Davies, E. C. Lightowlers, M. Stavola, K. Bergman, and B. Svensson, Phys. Rev. B **35**, 2755 (1987).
[25] L. D. Laude, F. H. Pollack, and M. Cardona, Phys. Rev. B **3**, 2623 (1971).
[26] G. Davies, E. C. Lightowlers, and M. C. Do Carmo, J. Phys. C **16**, 5503 (1983).
[27] C. P. Foy, J. Phys. C **15**, 2059 (1982).
[28] Z. Ciechanowska, G. Davies, and E. C. Lightowlers, Solid State Commun. **49**, 427 (1984).
[29] J. Wagner, A. Dornen, and R. Sauer, Phys. Rev. B **31**, 5561 (1985).
[30] G. Davies, E. C. Lightowlers, R. A. Woolley, R. C. Newman, and A. S. Oates, J. Phys. C **17**, L499 (1984).
[31] K. Thonke, G. D. Watkins, and R. Sauer, Solid State Commun. **51**, 127 (1984).
[32] E. Irion, K. Thonke, and R. Sauer, J. Phys. C **18**, 5069 (1985).
[33] A. N. Safonov, E. C. Lightowlers, G. Davies, P. Leary, R. Jones, and S. Öberg, Phys. Rev. Lett. **77**, 4812 (1996).
[34] A. N. Safonov, E. C. Lightowlers, and G. Davies, Mater. Sci. Forum **196**, 909 (1995).
[35] W. B. Fowler, *Physics of Color Centers* (Academic Press, New York, 1968).
[36] H. J. McSkimmin and P. Andreacht, J. Appl. Phys. **35**, 2161 (1964).
[37] A. A. Maraudin, Solid State Phys. **18**, 273 (1966).
[38] F. Rodríguez, M. Moreno, J. M. Dance, and A. Tressaud, Solid State Commun. **69**, 67 (1989).
[39] M. C. Marco de Lucas, F. Rodríguez, and M. Moreno, J. Phys.: Condens. Matter **7**, 7535 (1995).